

Experimental data from out-of-plane shake-table tests on unreinforced masonry gables

Earthquake Spectra

1–19

© The Author(s) 2025



Article reuse guidelines:

sagepub.com/journals-permissions

DOI: 10.1177/87552930251378248

journals.sagepub.com/home/eqs

Satyadhrik Sharma, M.EERI¹ ,
Nicolò Damiani^{2,3}, Marta Bertassi⁴,
Marco Smerilli³, Michele Mirra¹, Igor Lanese³,
Elisa Rizzo Parisi³, Gerard J O'Reilly, M.EERI⁴ ,
Francesco Messali, M.EERI¹, and
Francesco Graziotti^{2,3} 

Abstract

This article presents a dataset from an experimental campaign investigating the out-of-plane (OOP) seismic response of unreinforced masonry (URM) gables in existing buildings. Addressing a critical gap in published research, the dataset provides novel experimental data on the incremental dynamic OOP behavior of three URM gables tested under seismic loading until full collapse. All three gables were nominally identical but differed in their interaction with the supporting roof structure. This interaction was experimentally reproduced by imposing differential motions at the top of the gables, which were either linearly amplified or both amplified and phase-shifted relative to the motion at the base. This approach ensured idealized and numerically replicable boundary conditions, making the dataset an ideal benchmark for refining existing and developing new modeling approaches for URM structures. The dataset includes measured and calculated acceleration, displacement, and force time histories. Beyond supporting the validation and development of numerical models, it can also contribute to improving guidelines for the out-of-plane seismic assessment of URM gables and is openly available for further research and engineering applications.

¹Faculty of Civil Engineering and Geosciences, Delft University of Technology (TU Delft), Delft, The Netherlands

²Department of Civil Engineering and Architecture (DICA), University of Pavia, Pavia, Italy

³European Centre for Training and Research in Earthquake Engineering (EUCENTRE), Pavia, Italy

⁴University School for Advanced Studies IUSS Pavia, Pavia, Italy

Corresponding authors:

Satyadhrik Sharma, Faculty of Civil Engineering and Geosciences, Delft University of Technology (TU Delft), Stevinweg 1, 2628 CN Delft, The Netherlands.

Email: s.sharma@tudelft.nl

Nicolò Damiani, Department of Civil Engineering and Architecture (DICA), University of Pavia, via Ferrata 3, 27100 Pavia, Italy.

Email: nicolo.damiani@unipv.it

Keywords

Differential input motions, gable walls, incremental dynamic shake-table tests, roof stiffness, out of plane, unreinforced masonry

Date received: 8 April 2025; accepted: 13 July 2025

Introduction

Unreinforced masonry (URM) gables are among the most seismically vulnerable components of low-rise masonry buildings, as evidenced by numerous post-earthquake damage assessments. This vulnerability is attributed to their slender geometry, weak roof connections, and exposure to amplified seismic excitation at the building apex. Their interaction with flexible roof structures, such as timber roofs, further influences their seismic vulnerability. Despite this, dedicated experimental data on their out-of-plane (OOP) behavior remain scarce, with most insights derived from tests on complete buildings with gables (Graziotti et al., 2017; Guerrini et al., 2019; Kallioras et al., 2020, 2022; Magenes et al., 2014; Miglietta et al., 2021; Tomassetti et al., 2019a), or walls with rectangular geometries (Damiola et al., 2018; Giaretton et al., 2016; Graziotti et al., 2016; Griffith et al., 2004, 2007; Messali et al., 2017; Moshfeghi et al., 2024; Penner and Elwood, 2016; Sharma et al., 2020a, 2020b; Sharma et al., 2020; Tomassetti et al., 2019b; Vaculik and Griffith, 2018), rather than isolated gables. Among the limited tests focusing on gables, their interaction with the roof was either disregarded (Candeias et al., 2016) or the roof motion was not explicitly controlled (Tomassetti et al., 2019c), making them unsuitable to be adopted as experimental benchmarks for developing, refining, and validating numerical modeling strategies.

To address this, the ERIES (*Engineering Research Infrastructures for European Synergies*)-SUPREME (*Seismic oUt-of-Plane REsponse of Masonry gableEs*) Project was established as a joint initiative of Delft University of Technology (TU Delft), the Dutch Organisation for Applied Scientific Research (TNO), the University of Pavia, and the European Centre for Training and Research in Earthquake Engineering (EUCENTRE). The project aimed to improve the understanding of the seismic OOP response of URM gables in existing buildings in their as-built configuration without any retrofit or strengthening measures. Its primary objective was to generate experimental data which can be used as benchmarks for numerical model development on the dynamic behavior of URM gables, which had been largely missing from published literature. To achieve this, incremental dynamic tests were conducted to investigate the force and displacement capacity of URM gables under OOP seismic loading. A secondary objective was to quantify the influence of roof diaphragms on the gable OOP response, specifically how roof stiffness and the effectiveness of its connections to the gables influenced the seismic performance at different damage states. It should be noted that while retrofitting measures such as reinforced-concrete tie-columns or tie-beams and steel angles connecting roof joists to gables are known to improve the seismic performance of gables, the present study focuses exclusively on evaluating the baseline as-built behavior of URM gables against which the effectiveness of such retrofit measures can be quantified in future research.

As part of this project, a testing campaign involving the incremental dynamic testing of three full-scale URM gables until complete collapse was carried out as presented in Section “The experimental campaign.” While all three gables were nominally identical, they were subjected to different seismic inputs at their top and bottom to simulate

interaction with various roof typologies. The experimental specimens are described in Section “Tested URM gables.” The use of differential motions at the top and base of the gables to replicate roof interaction was enabled by an innovative test setup, detailed in Section “Test setup.” All three gables were heavily instrumented, with the instrumentation setup described in Section “Instrumentation.” The applied input motions and the adopted incremental dynamic sequence are presented in Section “Input seismic motions and incremental dynamic testing sequence.” This approach ensured idealized and numerically replicable boundary conditions, making the dataset a valuable benchmark for refining existing numerical modeling approaches for URM gables and developing new tools. This data paper ultimately presents the dataset obtained from these experiments in Section “The dataset,” providing both measured quantities (acceleration and displacement) and derived quantities (inertial force), each described in detail. The dataset, which includes the experimental data as well as video recordings of each experiment, is openly available for download from the Built Environment Data database at <https://doi.org/10.60756/euc-lavy7q49>. Finally, the concluding remarks are summarized in Section “Concluding remarks.”

The experimental campaign

The experimental campaign of the ERIES-SUPREME project involved the incremental dynamic testing of three full-scale URM gables until complete collapse. The tests were conducted at the EUCENTRE laboratory in Pavia, Italy, using the 9DLAB facility. This advanced seismic testing system features a dual shake-table setup, where the top and bottom tables can apply differential input motions across nine degrees of freedom. While the 9D LAB, with its in-plane dimensions of 4.8×4.8 m, allowed for full-scale masonry gable testing, it could not accommodate an entire roof diaphragm. To account for the influence of roof stiffness on the gable response, variations in the input motion applied to the top table were introduced. Specifically, three different roof configurations were considered within the same experimental campaign: a stiff roof (Gable1-STIFF), a semi-rigid roof (Gable2-SEMIFLEX), and a flexible roof (Gable3-FLEX). The input motions applied at the bottom table were identical for all three gables, while the motion at the top table varied for each specimen:

- Gable1-STIFF: The motion at the top and bottom tables was the same, simulating interaction with a stiff roof diaphragm.
- Gable2-SEMIFLEX: The motion at the top table was linearly amplified relative to the bottom table, simulating interaction with a semi-rigid roof diaphragm.
- Gable3-FLEX: The motion at the top table was both amplified and out of phase with the bottom table, representing interaction with a flexible roof diaphragm.

Tested URM gables

The tested specimens were identical full-scale URM gable walls with a triangular shape, a base length of 6 m, and a height of 3 m (Figure 1). They were constructed on a composite steel-concrete foundation. Each gable was built using solid clay bricks with average dimensions of $230 \times 105 \times 55$ mm, resulting in a wall thickness of 105 mm. The masonry was laid in 45 courses with 10-mm-thick mortar joints. In addition, five joist pockets were incorporated to accommodate timber beams with a cross-section of 100×200 mm. Each

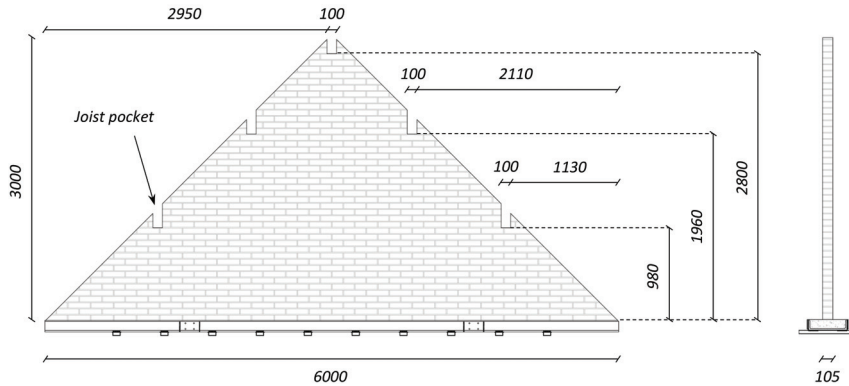


Figure 1. Geometry of the tested URM gables (units of mm).

beam was subjected to an approximate load of 4.5 kN, simulating the vertical load exerted by the roof diaphragm, leading to a total vertical load of 22.5 kN on the gable. This load is representative of half the weight of a roof diaphragm, consistent with the geometry of the specimen. The tested gable represents one of two end gables in a roof structure where the total roof weight is shared equally, with each gable bearing half of the load. The beams also facilitated the application of lateral loads along the specimen height, as detailed in the following sections. The timber-to-masonry connections relied solely on friction, with the timber joists placed into the joist pockets to their full depth only after the masonry had fully cured. Mechanical characterization of all specimen materials was conducted and is also accessible at <https://doi.org/10.60756/euc-1avy7q49>.

Test setup

The experimental setup featured a dual shake-table configuration, with a top and bottom table designed to apply differential input motions (Figure 2). A custom steel loading frame was constructed to transmit accelerations along the height of the gable through five horizontal loading arms, each hinged to the frame. Timber beams were attached to the steel arms using screws to replicate the behavior of timber joists commonly found in real roof structures.

To prevent any unintended increase in out-of-plane stiffness and strength, the loading frame was hinged at both the top and bottom shake tables. The gable foundations were securely fixed to the bottom shake table using steel bolts. A rigid instrumentation frame, anchored to the bottom shake table, completed the setup, providing a fixed reference point for measurements and supporting the instrumentation system.

A system of five springs, one per loading arm, was used to apply vertical loads that simulated the weight of the roof. These vertical loads were applied by pulling down the horizontal steel arms with steel bars connected in series with the springs. The stiffness of the springs (≈ 50 N/mm) was calibrated to prevent excessive increases in the vertical load applied to the timber beams, even as the gable approached collapse. Deformations and the corresponding vertical loads exerted by the springs on the timber beams were continuously monitored throughout testing, providing essential data to support numerical modeling of these benchmark experiments.

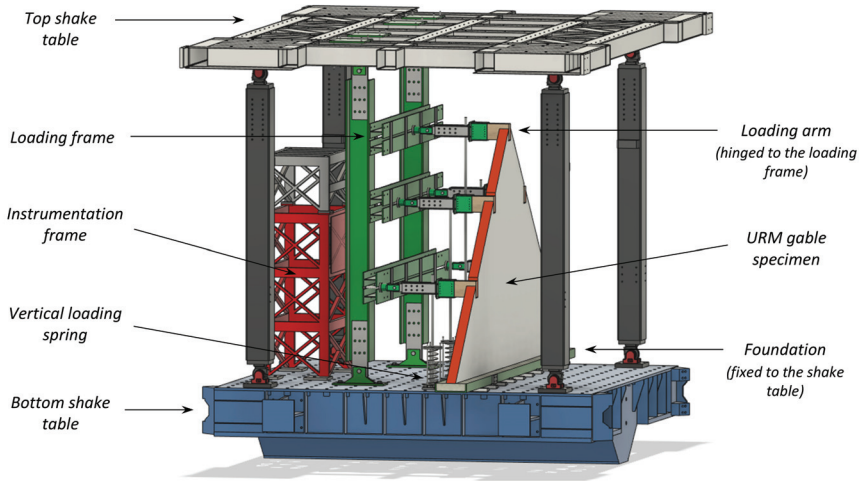


Figure 2. Three-dimensional view of the testing setup.

Instrumentation

The instrumentation for each specimen included accelerometers, traditional potentiometers, wire potentiometers, and a 3D optical acquisition system. Instrument placement was determined based on the expected deformed shapes and cracking patterns of the gables. Accelerometers were installed on the gable specimens to record acceleration-time histories, with additional units placed on the loading and instrumentation frames, as well as on the specimen foundation. The accelerometers used were silicon Micro-Electro-Mechanical Systems (MEMS)-based devices with a nominal bandwidth of 0–200 Hz. Traditional potentiometers measured the elongation or shortening of the springs and the relative displacements between the timber beams and the masonry. Wire potentiometers, mounted on both the loading and instrumentation frames, recorded gable displacements. The optical monitoring system played a crucial role in maintaining dense instrumentation during high-intensity shake-table tests, when some traditional instruments had to be removed to prevent collateral damage. It was used to measure displacements on the free surface of the gable, opposite to the loading frame, ensuring continuous and detailed data acquisition. This comprehensive instrumentation scheme (illustrated for each of the three specimens in Figure 3) resulted in 165 different time histories of displacements and accelerations recorded for the gables until their complete collapse. The numbers shown in Figure 3 correspond to the instrument identifiers used for dataset organization, as explained in more detail in Section “The dataset.”

Input seismic motions and incremental dynamic testing sequence

The input motions applied at the top and bottom tables were selected to represent two alternative floor motions (FM) scenarios: induced seismicity and tectonic seismicity. For the induced seismicity scenario (FM1), finite element-based numerical analyses were conducted on a typical URM building from the Groningen region of the Netherlands. The analyses considered the building in its as-built condition with a flexible timber roof, as well as in two retrofitted configurations: one with a stiff concrete roof and another with a semi-flexible timber-strengthened roof. For the tectonic seismicity scenario (FM2), input

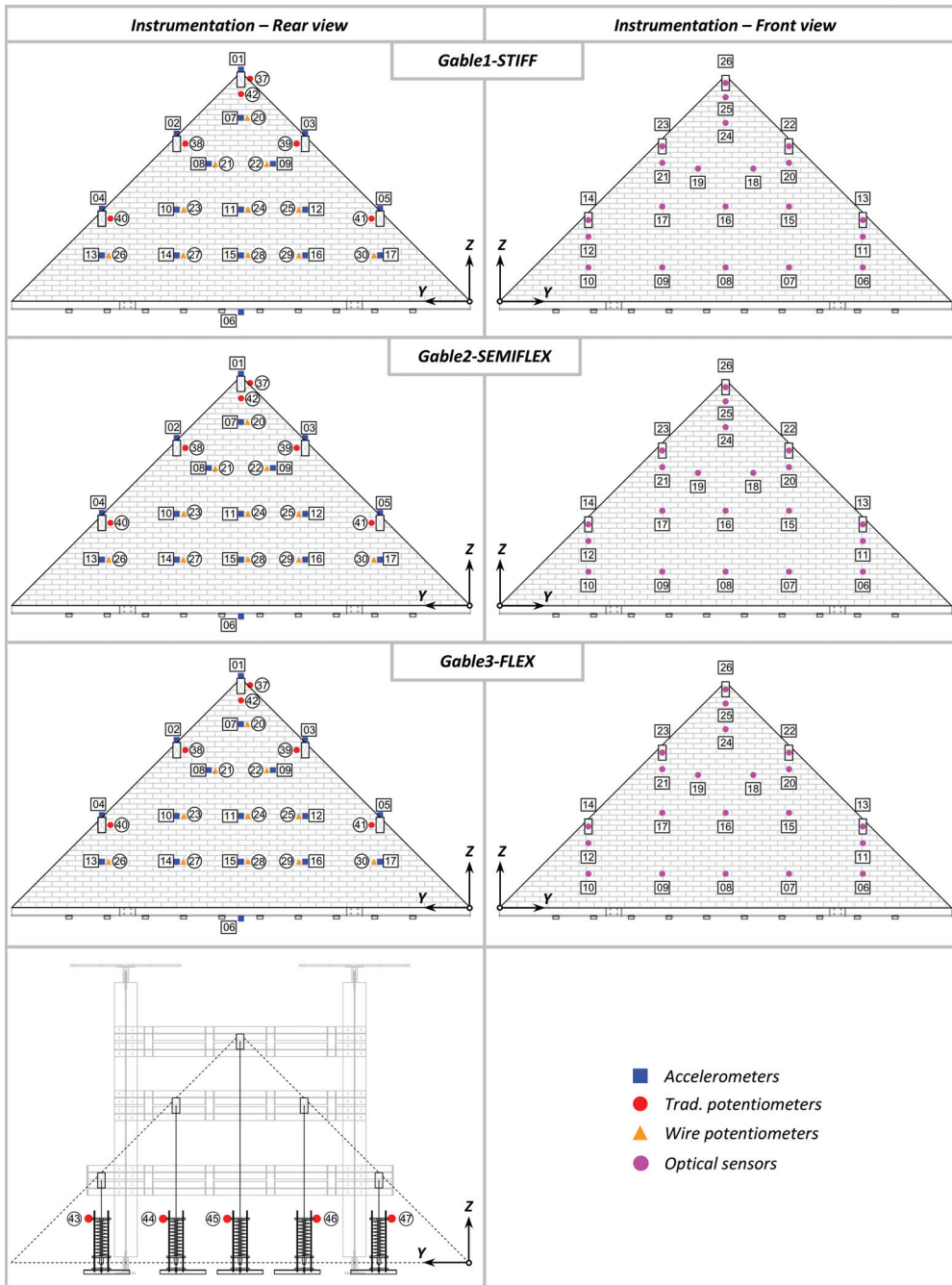


Figure 3. Rear and front views of the instrumentation used for Gable1-STIFF, Gable2-SEMIFLEX, and Gable3-FLEX.

motions were derived from recordings of the 2016 Central Italy earthquake, obtained from a monitored masonry building at the attic floor level. In this case, the gable-roof interaction was modeled using a representative elastic single-degree-of-freedom system, featuring

a fundamental mode of vibration with a period of 0.5 s and a damping ratio of 5%. Further details on the selection of input signals can be found in Mirra et al. (2025).

All three gables were tested using an incremental dynamic approach, where the input motions on both the top and bottom shake tables were linearly scaled by a scaling factor (SF) until complete collapse. The testing sequence applied to each gable, including the scaling factors (SF), peak base acceleration (PBA), and peak ridge acceleration (PRA), is summarized in Table 1. It should be noted that for Gable3-FLEX, an additional shake-table test at 100% FM1 was conducted after Test #9 (i.e. the 100% FM2 run) to evaluate its ability to withstand an induced seismic motion corresponding to the highest PBA expected as per the current hazard model for Groningen, the Netherlands after sustaining damage from tectonic motion.

The dataset

The data from the experimental campaign is provided in .txt/.csv files, with each column containing either measured or computed data. A separate .txt/.csv file is available for each test, with filenames indicating the corresponding test (Table 1). Videos of each run in the testing sequence are also included in the shared directory which can be downloaded at <https://doi.org/10.60756/euc-lavy7q49>. All acquired data were filtered for frequencies above 48 Hz. Displacements are expressed in [mm], accelerations in [m/s^2], and forces in [kN]. Note that the displacement measurements include residual values, as the displacements recorded were intentionally not reset to zero at the end of each testing run in the testing sequence (Table 1). When instruments were offline, their values are recorded as “not a number” (NaN), including during the final part of the last run after the specimen had collapsed.

Organization of the data

The organization of the .txt/.csv files, specifically the data stored in each column, is summarized in Tables 2 to 4 for Gable1-STIFF as an example. The same tables for Gable2-SEMI-FLEX and Gable3-FLEX are available for download at <https://doi.org/10.60756/euc-lavy7q49>. In these tables, the “Col.” column refers to the column number in the data matrix, while “Instr. No.” indicates the instrument number in Figure 3. The “Type” column specifies the instrument type, which can be an accelerometer (ACC), traditional potentiometer (TP), wire potentiometer with 1000 mm maximum elongation (WP LONG), wire potentiometer with 250 mm maximum elongation (WP SHORT), and optical measurement (OPT). In addition, the dataset includes the directly measured acceleration, velocity and displacement readouts (READOUT) from both the top and bottom shake tables, and computed data (COMPUTED), such as inertial force or control point displacement. The “Description” column provides a brief explanation of the instrument location, and the “Offline” column lists the test numbers during which the instrument was not recording. The “Dir.” column indicates the measurement direction, while Location refers to the instrument coordinates in the gable plane. Finally, “Area T#” and “Mass T#” correspond to the area distribution and mass values assigned in test T#, respectively. These values are used to compute the inertial force associated with the URM gable, as detailed in Section “Computed data,” and are included in the dataset.

All optical measurements are post-processed to be relative to the base/lower shake table. Potentiometers measure relative displacements between the two locations they are

Table 1. Incremental dynamic testing sequence of three specimens (Nom: nominal; Rec: recorded; PBA: peak base acceleration; PRA: peak ridge acceleration)

Test #	SF	Gable1-STIFF				Gable2-SEMIFLEX				Gable3-FLEX			
		PBA [g]		PRA [g]		PBA [g]		PRA [g]		PBA [g]		PRA [g]	
		Nom.	Rec.	Nom.	Rec.	Nom.	Rec.	Nom.	Rec.	Nom.	Rec.	Nom.	Rec.
1	FMI	0.04	0.05	0.04	0.13	0.04	0.05	0.08	0.16	0.04	0.05	0.12	0.31
2		0.08	0.08	0.08	0.19	0.08	0.08	0.16	0.29	0.08	0.09	0.24	0.53
3		0.13	0.12	0.13	0.26	0.13	0.12	0.23	0.36	0.13	0.13	0.36	0.55
4		0.21	0.19	0.21	0.39	0.21	0.20	0.39	0.45	0.21	0.20	0.60	0.84
5		0.32	0.28	0.32	0.49	0.32	0.28	0.58	0.62	0.32	0.28	0.90	1.10
6		0.42	0.37	0.42	0.61	0.42	0.38	0.78	0.81	0.42	0.36	1.20	1.33
7	FM2	0.27	0.29	0.27	0.44	0.27	0.28	0.43	0.62	0.27	0.28	0.65	0.79
8		0.41	0.43	0.41	0.53	0.41	0.42	0.64	0.93	0.41	0.43	0.97	1.28
9		0.55	0.57	0.55	0.71	0.55	0.57	0.85	1.26	0.55	0.57	1.30	1.91
10		0.69	0.69	0.69	0.84	0.69	0.71	1.06	1.46	0.69	0.36	1.20	1.33
11		0.82	0.86	0.82	0.96	0.82	0.86	1.28	1.86	0.82	0.70	1.62	2.34
12		0.96	1.03	0.96	1.19	0.96	1.00	1.49	2.15	0.96	0.85	1.95	2.56
13		1.10	1.17	1.10	1.34	1.10	1.04	1.70	3.31	-	-	-	-
14		1.38	1.51	1.38	1.64	-	-	-	-	-	-	-	-
15		1.65	1.88	1.65	1.86	-	-	-	-	-	-	-	-
16		1.93	1.80	1.93	2.56	-	-	-	-	-	-	-	-

Table 2. Organization of the experimentally measured acceleration data for GableI-STIFF

Col.	Instr. No.	Type	Description	Offline	Dir.	Location		Area T1 ÷ T13	Mass T1 ÷ T13	Area T14 ÷ T16	Mass T14 ÷ T16
						Y [mm]	Z [mm]	[m ²]	[kg]	[m ²]	[kg]
1	-	-	Time [s]	-	-	-	-	-	-	-	-
Accelerometers											
2	1	ACC	Ridge Beam Acceleration (top) [m/s ²]	-	X	3000	3000	-	-	0.20	39.16
3		ACC			Y			-	-	-	-
4		ACC			Z			-	-	-	-
5	2	ACC	Load-bearing Beam Acceleration (middle) [m/s ²]	-	X	2160	2160	-	-	0.82	161.95
6		ACC			Y			-	-	-	-
7		ACC			Z			-	-	-	-
8	3	ACC	Load-bearing Beam Acceleration (middle) [m/s ²]	-	X	3840	2160	-	-	0.82	161.95
9		ACC			Y			-	-	-	-
10		ACC			Z			-	-	-	-
11	4	ACC	Load-bearing Beam Acceleration (bottom) [m/s ²]	-	X	1180	1180	-	-	-	-
12		ACC			Y			-	-	-	-
13		ACC			Z			-	-	-	-
14	5	ACC	Load-bearing Beam Acceleration (bottom) [m/s ²]	-	X	4820	1180	-	-	-	-
15		ACC			Y			-	-	-	-
16		ACC			Z			-	-	-	-
17	6	ACC	Shake Table [m/s ²]	-	X	3000	-150	1.71	338.44	3.07	607.23
18		ACC			Y			-	-	-	-
19		ACC			Z			-	-	-	-
20	7	ACC	Gable Wall Acceleration [m/s ²]	T14,T15,T16	X	3000	2400	0.81	160.17	-	-
21		ACC			Y			-	-	-	-
22		ACC			Z			-	-	-	-
23	8	ACC	Gable Wall Acceleration [m/s ²]	T14,T15,T16	X	2580	1800	0.72	142.38	-	-
24		ACC			Y			-	-	-	-
25		ACC			Z			-	-	-	-
26	9	ACC	Gable Wall Acceleration [m/s ²]	T14,T15,T16	X	3420	1800	0.72	142.38	-	-
27		ACC			Y			-	-	-	-
28		ACC			Z			-	-	-	-
29	10	ACC	Gable Wall Acceleration [m/s ²]	T14,T15,T16	X	2000	1200	0.55	107.97	-	-
30		ACC			Y			-	-	-	-
31		ACC			Z			-	-	-	-
32	11	ACC	Gable Wall Acceleration [m/s ²]	-	X	3000	1200	0.50	99.66	4.09	809.41
33		ACC			Y			-	-	-	-
34		ACC			Z			-	-	-	-

(continued)

Table 2. Continued

Col.	Instr. No.	Type	Description	Offline	Dir.	Location		Area T1 ÷ T13 [m ²]	Mass T1 ÷ T13 [kg]	Area T14 ÷ T16 [m ²]	Mass T14 ÷ T16 [kg]
						Y [mm]	Z [mm]				
35	12	ACC	Gable Wall Acceleration [m/s ²]	T15,T16	X	4000	1200	0.55	107.97	-	-
36	36	ACC			Y	-	-	-	-	-	-
37	37	ACC			Z	-	-	-	-	-	-
38	13	ACC	Gable Wall Acceleration [m/s ²]	T15,T16	X	1250	550	0.92	182.72	-	-
39	39	ACC			Y	-	-	-	-	-	-
40	40	ACC			Z	-	-	-	-	-	-
41	14	ACC	Gable Wall Acceleration [m/s ²]	T14,T15,T16	X	2200	550	0.55	107.97	-	-
42	42	ACC			Y	-	-	-	-	-	-
43	43	ACC			Z	-	-	-	-	-	-
44	15	ACC	Gable Wall Acceleration [m/s ²]	T14,T15,T16	X	3000	550	0.50	99.66	-	-
45	45	ACC			Y	-	-	-	-	-	-
46	46	ACC			Z	-	-	-	-	-	-
47	16	ACC	Gable Wall Acceleration [m/s ²]	T14,T15,T16	X	3800	550	0.55	107.97	-	-
48	48	ACC			Y	-	-	-	-	-	-
49	49	ACC			Z	-	-	-	-	-	-
50	17	ACC	Gable Wall Acceleration [m/s ²]	T14,T15,T16	X	4750	550	0.92	182.72	-	-
51	51	ACC			Y	-	-	-	-	-	-
52	52	ACC			Z	-	-	-	-	-	-
53	18	ACC	Loading frame behind top hinge [m/s ²]	-	X	-	-	-	-	-	-
54	54	ACC			Y	-	-	-	-	-	-
55	55	ACC			Z	-	-	-	-	-	-
56	19	ACC	Instrumentation frame [m/s ²]	-	X	-	-	-	-	-	-
57	57	ACC			Y	-	-	-	-	-	-
58	58	ACC			Z	-	-	-	-	-	-

connected to, which are specified in Table 3. The sign conventions for each instrument type are as follows. For accelerometers (ACC) and optical measurements (OPT), a positive sign (+) indicates movement toward the loading frame ($-x$), while a negative sign ($-$) represents movement away from the loading frame ($+x$). For traditional potentiometers (TP) and wire potentiometers (WP), a positive sign (+) corresponds to elongation ($+x$), whereas a negative sign ($-$) indicates shortening ($-x$).

Computed data

In addition to the measured data, the dataset includes two computed quantities: (1) the displacement of a control point and (2) the inertial force associated with the gable at each stage of the incremental dynamic testing. This section outlines the procedure adopted to compute these quantities. Plotting inertial force against control point displacement allows for the evaluation of the gable hysteretic force-displacement response.

1. **Control Point Displacement:** Although the gables were densely instrumented, the location experiencing the maximum displacement was not always directly measured. To address this, a computed control point displacement is included in the dataset, representing the maximum deflection experienced by the URM gable in each test. The location of this control point varied as damage evolved and was selected based on both primary and secondary deformation mechanisms. All control point displacements reflect the actual gable deformation, excluding any rigid-body displacement from the loading frame. In the early stages of testing, prior to the development of the collapse mechanism, the control point was assumed at the midpoint of the gable, at a height of 1200 mm from the base, corresponding to the position of wire potentiometer No. 24 (see Figure 3, Table 3). In the final test runs, once the collapse mechanism had developed, the control point was relocated to correspond with the red marker shown in Figure 4 for each gable. In the same figure, the test numbers (Test #) indicate the tests for which the control point displacement was computed using the position of the red marker.
2. **Inertial Force:** Time histories of inertial forces were computed by multiplying the accelerations recorded by the accelerometers by the corresponding tributary masses, assuming the mass was lumped at the accelerometer locations. The initial tributary area distribution was consistent across the three masonry gables. However, as testing progressed, the tributary masses were updated to reflect damage progression and crack patterns. These adjustments also took into account the presence or removal of accelerometers, as redundant instruments were removed during higher-intensity tests or when the gable was severely damaged, in order to minimize the risk of equipment loss. Note that for Gable3-FLEX, in order to ensure a mass distribution as consistent as possible with the observed failure mechanism, the displacement recorded by optical marker No. 24 was used to estimate the corresponding acceleration (not included in the dataset), to which the associated mass was then assigned. Details on the area assigned to each accelerometer throughout the testing sequence for all three gables are provided in Figure 5. The values associated with these areas for Gable1-STIFF are provided in Table 2 while the same for Gable2-SEMIFLEX and Gable3-FLEX are available for download at <https://doi.org/10.60756/euc-1avy7q49>.

Table 3. Organization of the experimentally measured displacement data for Gable I-STIFF

Col.	Instr. No.	Type	Description	Offline	Dir:	Location	
						Y [mm]	Z [mm]
I	-	-	Time [s]	-	-	-	-
Wire Potentiometers							
59	20	WP LONG	Gable Wall Displacement—Instrum. frame [mm]			3000	2400
60	21	WP LONG	Gable Wall Displacement—Instrum. frame [mm]	X	X	2580	1800
61	22	WP LONG	Gable Wall Displacement—Instrum. frame [mm]			3420	1800
62	23	WP SHORT	Gable Wall Displacement—Loading frame [mm]	X	X	2000	1200
63	24	WP SHORT	Gable Wall Displacement—Loading frame [mm]	X	X	3000	1200
64	25	WP SHORT	Gable Wall Displacement—Loading frame [mm]	X	X	4000	1200
65	26	WP SHORT	Gable Wall Displacement—Shake table support [mm]	X	X	1250	550
66	27	WP SHORT	Gable Wall Displacement—Instrum. frame [mm]	X	X	2200	550
67	28	WP SHORT	Gable Wall Displacement—Instrum. frame [mm]	X	X	3000	550
68	29	WP SHORT	Gable Wall Displacement—Instrum. frame [mm]	X	X	3800	550
69	30	WP SHORT	Gable Wall Displacement—Shake table support [mm]	X	X	4750	550
70	36	WP SHORT	Lower Steel Beam (Load. frame)—Instrum. frame [mm]	X	X	3000	1064
71	48	WP LONG	Upper Steel Beam (Load. frame)—Instrum. frame [mm]	X	X	3000	2704
Traditional Potentiometers							
72	37	TP	Load-bearing Beam—Gable Displacement (top) [mm]				
73	38	TP	Load-bearing Beam—Gable Displacement (middle) [mm]	X	X	-	-
74	39	TP	Load-bearing Beam—Gable Displacement (middle) [mm]	X	X	-	-
75	40	TP	Load-bearing Beam—Gable Displacement (bottom) [mm]	X	X	-	-
76	41	TP	Load-bearing Beam—Gable Displacement (bottom) [mm]	X	X	-	-
77	42	TP	Ridge Beam—Gable hollow, transversal displacement [mm]	Y	Y	-	-
78	43	TP	Spring Displacement [mm]	Z	Z	-	-
79	44	TP	Spring Displacement [mm]	Z	Z	-	-
80	45	TP	Spring Displacement [mm]	Z	Z	-	-
81	46	TP	Spring Displacement [mm]	Z	Z	-	-
82	47	TP	Spring Displacement [mm]	Z	Z	-	-
Optical Markers							
83	I	OPT	Marker Displacement of bottom table [mm]			-	-
84		OPT		X	Y		
85		OPT		Z	Z		
86	6	OPT	Marker Displacement [mm]	X	X	4760	583
87		OPT		Y	Y		
88		OPT		Z	Z		

(continued)

Table 3. Continued

Col.	Instr. No.	Type	Description	Offline	Dir:	Location	
						Y [mm]	Z [mm]
89	7	OPT	Marker Displacement [mm]	-	X	3800	583
90		OPT			Y		
91		OPT			Z		
92	8	OPT	Marker Displacement [mm]	-	X	3000	583
93		OPT			Y		
94		OPT			Z		
95	9	OPT	Marker Displacement [mm]	-	X	2200	583
96		OPT			Y		
97		OPT			Z		
98	10	OPT	Marker Displacement [mm]	-	X	1240	583
99		OPT			Y		
100		OPT			Z		
101	11	OPT	Marker Displacement [mm]	-	X	4823	908
102		OPT			Y		
103		OPT			Z		
104	12	OPT	Marker Displacement [mm]	-	X	1177	908
105		OPT			Y		
106		OPT			Z		
107	13	OPT	Marker Displacement of beam (bottom) [mm]	-	X	4823	1119
108		OPT			Y		
109		OPT			Z		
110	14	OPT	Marker Displacement of beam (bottom) [mm]	-	X	1177	1119
111		OPT			Y		
112		OPT			Z		
113	15	OPT	Marker Displacement [mm]	-	X	3960	1239
114		OPT			Y		
115		OPT			Z		
116	16	OPT	Marker Displacement [mm]	-	X	3000	1239
117		OPT			Y		
118		OPT			Z		
119	17	OPT	Marker Displacement [mm]	-	X	2040	1239
120		OPT			Y		
121		OPT			Z		

(continued)

Table 3. Continued

Col.	Instr. No.	Type	Description	Offline	Dir.	Location	
						Y [mm]	Z [mm]
122	18	OPT	Marker Displacement [mm]	-	X	3355	1827
123		OPT			Y		
124		OPT			Z		
125	19	OPT	Marker Displacement [mm]	-	X	2645	1827
126		OPT			Y		
127		OPT			Z		
128	20	OPT	Marker Displacement [mm]	-	X	3840	1903
129		OPT			Y		
130		OPT			Z		
131	21	OPT	Marker Displacement [mm]	-	X	2160	1903
132		OPT			Y		
133		OPT			Z		
134	22	OPT	Marker Displacement of beam (middle) [mm]	-	X	3840	2094
135		OPT			Y		
136		OPT			Z		
137	23	OPT	Marker Displacement of beam (middle) [mm]	-	X	2160	2094
138		OPT			Y		
139		OPT			Z		
140	24	OPT	Marker Displacement [mm]	-	X	3000	2418
141		OPT			Y		
142		OPT			Z		
143	25	OPT	Marker Displacement [mm]	-	X	3000	2759
144		OPT			Y		
145		OPT			Z		
146	26	OPT	Marker Displacement of beam (top) [mm]	-	X	3000	2948
147		OPT			Y		
148		OPT			Z		
149	27	OPT	Marker Displacement Loading frame[mm]	-	X	-	-
150		OPT			Y		
151		OPT			Z		
152	28	OPT	Marker Displacement Loading frame [mm]	-	X	-	-
153		OPT			Y		
154		OPT			Z		
155	29	OPT	Marker Displacement Loading frame [mm]	-	X	-	-
156		OPT			Y		
157		OPT			Z		

Table 4. Organization of the shake-table measurements (read out) and computed data for GableI-STIFF

Col.	Type	Description	Offline	Dir.
1	-	Time [s]	-	-
Shake-Table Measurements				
158	READOUT	Bottom Acceleration [m/s^2]	-	X
159	READOUT	Top Acceleration [m/s^2]	-	X
160	READOUT	Bottom Displacement [mm]	-	X
161	READOUT	Top Displacement [mm]	-	X
162	READOUT	Bottom Acceleration [m/s^2]	-	Y
163	READOUT	Top Acceleration [m/s^2]	-	Y
164	READOUT	Bottom Displacement [mm]	-	Y
165	READOUT	Top Displacement [mm]	-	Y
Computed Data				
166	COMPUTED	Inertial Force [kN]	-	X
167	COMPUTED	Control Point Displacement [mm]	-	X

Data organization and illustrative examples

All data are available at <https://doi.org/10.60756/euc-1avy7q49> and are provided in a ZIP archive together with a detailed technical report. The archive comprises two directories, “Videos” and “TXT,” each of which contains three subdirectories corresponding to the three tested gables. Within each subdirectory, the video files and .txt data files are named according to the specific run of the incremental dynamic testing sequence (see Table 1). Their file names reflect the run number in the testing sequence, the motion used and the associated scaling factor. The following are specific examples of how to interpret a .txt in the experimental dataset:

1. Instrument No. 1 (Figure 3) is an accelerometer (ACC), stored in columns 2,3 and 4 (Table 2) of the .txt files measures accelerations on the ridge beam. It remained online and recorded every test of GableI-STIFF.
2. Instrument No. 20 (Figure 3) is a wire potentiometer with 250 mm elongation (WP SHORT), stored in column 59 (Table 3) of the .txt files measures relative displacements between the instrumentation frame (Figure 2) and the upper part of the gable ($X = 3000$ mm, $Z = 2400$ mm).
3. Instrument No. 37 (Figure 3) is a traditional potentiometer (TP), stored in column 72 (Table 3) of the .txt files measures relative displacements between the ridge beam and the gable. It was offline (not recording) during Test #14, Test #15, and Test #16 (Table 2) for GableI-STIFF.
4. Instruments No. 43 to 47 (Figure 3), stored in columns 78 to 82 (Table 3) of the .txt files, measure the displacements of the springs applying vertical force to the purlins. Negative displacements indicate an increase in the applied vertical force relative to the target vertical load on the purlins. Positive displacements indicate a reduction in vertical force relative to the target vertical load.

Concluding remarks

This dataset provides comprehensive experimental data from incremental dynamic shake-table tests on three full-scale unreinforced masonry (URM) gables, offering valuable insights into their out-of-plane seismic response. The dataset includes measured and

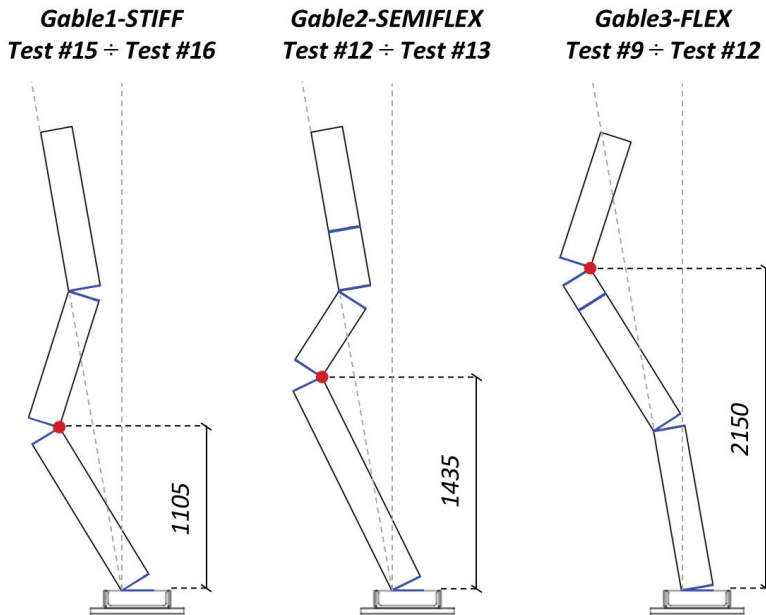


Figure 4. Location of the control points (red marker) for Gable1-STIFF, Gable2-SEMIFLEX, and Gable3-FLEX after the development of the collapse mechanism, with the corresponding test numbers indicated (units of mm).

computed quantities, such as accelerations, displacements, inertial forces, and control point displacements, recorded until complete collapse. The instrumentation strategy, along with adjustments made based on damage progression, ensures high-quality data suitable for benchmarking numerical models and refining seismic assessment guidelines. To support users in interpreting the dataset, illustrative examples are provided, detailing specific instrument readings and their significance within the experimental setup. In addition, videos of each test are available in the dataset, offering a visual reference for the observed structural response throughout the testing sequence. The dataset is openly available for download from the Built Environment Data database at <https://doi.org/10.60756/euc-lavy7q49>.

Declaration of conflicting interests

The author(s) declared no potential conflicts of interest with respect to the research, authorship, and/or publication of this article.

Funding

The author(s) disclosed receipt of the following financial support for the research, authorship, and/or publication of this article: The work presented in the present report is part of the transnational access project “ERIES-SUPREME,” supported by the Engineering Research Infrastructures for European Synergies (ERIES) project (www.eries.eu), which has received funding from the European Union’s Horizon Europe Framework Programme under Grant Agreement No. 101058684. This is ERIES publication number D6. Additional funding beyond the scope of ERIES was provided by the Ministry of Economic Affairs and Climate (Ministerie van Economische Zaken, EZK) through

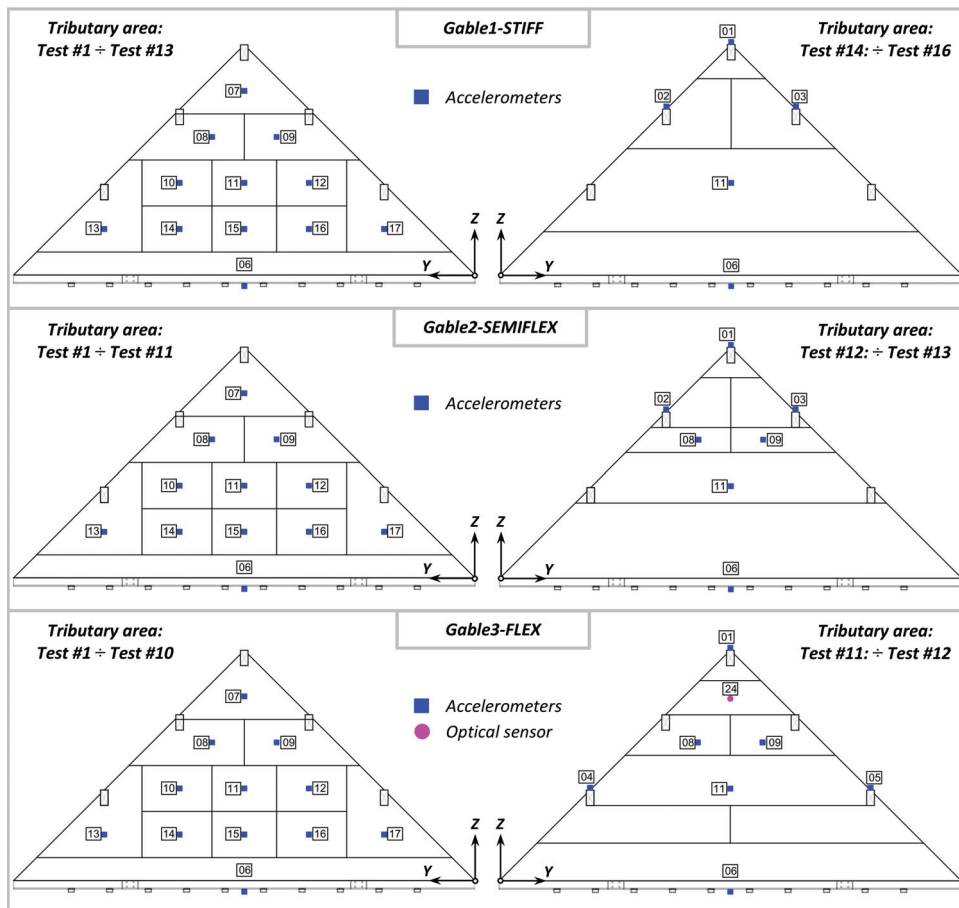





Figure 5. Tributary area/mass distribution used for calculating the inertial force for Gable1-STIFF, Gable2-SEMIFLEX, and Gable3-FLEX.

the Netherlands Organisation for Applied Scientific Research (TNO), under contract number 3100404105 “Wandenaanpak/TU Delft.”

ORCID iDs

Satyadhrik Sharma  <https://orcid.org/0000-0002-8965-5593>
 Gerard J O'Reilly  <https://orcid.org/0000-0001-5497-030X>
 Francesco Graziotti  <https://orcid.org/0000-0002-0223-0139>

Data availability statement

The dataset presented in this article is openly available for download from the Built Environment Data database at <https://doi.org/10.60756/euc-lavy7q49>.

Supplemental material

Supplemental material for this article is available online.

References

- Candeias PX, Costa AC, Mendes N, Costa AA and Lourenço PB (2016) Experimental assessment of the out-of-plane performance of masonry buildings through shaking table tests. *International Journal of Architectural Heritage*, pp. 1–28. DOI: 10.1080/15583058.2016.1238975.
- Damiola M, Esposito R, Messali F and Rots J (2018) Quasi-static cyclic two-way out-of-plane bending tests and analytical models comparison for URM walls. In: Milani G, Taliervo A and Garrity S (eds) *Proceeding of the 10th International Masonry Conference*. Milan.
- Giaretton M, Dizhur D and Ingham JM (2016) Dynamic testing of as-built clay brick unreinforced masonry parapets. *Engineering Structures* 127: 676–685.
- Graziotti F, Tomassetti U, Kallioras S, Penna A and Magenes G (2017) Shaking table test on a full scale URM cavity wall building. *Bulletin of Earthquake Engineering* 15(12): 5329–5364.
- Graziotti F, Tomassetti U, Penna A and Magenes G (2016a) Out-of-plane shaking table tests on URM single leaf and cavity walls. *Engineering Structures* 125: 455–470.
- Griffith MC, Lam NTK, Wilson JL and Doherty K (2004) Experimental investigation of unreinforced brick masonry walls in flexure. *Journal of Structural Engineering* 130(3): 423–432.
- Griffith MC, Vaculik J, Lam NTK, Wilson J and Lumantarna E (2007) Cyclic testing of unreinforced masonry walls in two-way bending. *Earthquake Engineering & Structural Dynamics* 36(6): 801–821.
- Guerrini G, Senaldi I, Graziotti F, Magenes G, Beyer K and Penna A (2019) Shake-table test of a strengthened stone masonry building aggregate with flexible diaphragms. *International Journal of Architectural Heritage* 13(7): 1078–1097.
- Kallioras S, Correia AA, Graziotti F, Penna A and Magenes G (2020) Collapse shake-table testing of a clay-URM building with chimneys. *Bulletin of Earthquake Engineering* 18(3): 1009–1048.
- Kallioras S, Graziotti F, Penna A and Magenes G (2022) Effects of vertical ground motions on the dynamic response of URM structures: Comparative shake-table tests. *Earthquake Engineering & Structural Dynamics* 51(2): 347–368.
- Magenes G, Penna A, Senaldi IE, Rota M and Galasco A (2014) Shaking table test of a strengthened full-scale stone masonry building with flexible diaphragms. *International Journal of Architectural Heritage* 8(3): 349–375.
- Messali F, Ravenshorst G, Esposito R and Rots JG (2017) Large-scale testing program for the seismic characterization of Dutch masonry walls. In: *Proceedings of the 16th World Conference on Earthquake Engineering (WCEE)*, Santiago, Chile.
- Miglietta M, Damiani N, Guerrini G and Graziotti F (2021) Full-scale shake-table tests on two unreinforced masonry cavity-wall buildings: Effect of an innovative timber retrofit. *Bulletin of Earthquake Engineering* 19(6): 2561–2596.
- Mirra M, Damiani N, Sharma S, Graziotti F and Messali F (2025) Definition of differential seismic input motions for out-of-plane dynamic testing of unreinforced masonry gable walls considering different roof configurations. *Structures* 79: 109419.
- Moshfeghi A, Smyrou E, Arslan O and Engin Bal I (2024) Out-of-plane shake table tests on solid masonry walls with timber floors. *Structures* 66: 106815.
- Penner O and Elwood KJ (2016.) Out-of-plane dynamic stability of unreinforced masonry walls in one-way bending: Parametric study and assessment guidelines. *Earthquake Spectra* 32(3): 1699–1723.
- Sharma S, Grottoli L, Tomassetti U and Graziotti F (2020) Dataset from shake-table testing of four full-scale URM walls in a two-way bending configuration subjected to combined out-of-plane horizontal and vertical excitation. *Data in Brief* 31: 105851.
- Sharma S, Tomassetti U, Grottoli L and Graziotti F (2020) Two-way bending experimental response of URM walls subjected to combined horizontal and vertical seismic excitation. *Engineering Structures* 219: 110537.
- Tomassetti U, Correia AA, Candeias PX, Graziotti F and Campos Costa A (2019a) Two-way bending out-of-plane collapse of a full-scale URM building tested on a shake table. *Bulletin of Earthquake Engineering* 17(4): 2165–2198.

- Tomassetti U, Correia AA, Graziotti F and Penna A (2019b) Seismic vulnerability of roof systems combining URM gable walls and timber diaphragms. *Earthquake Engineering & Structural Dynamics* 48(11): 1297–1318.
- Tomassetti U, Grottoli L, Sharma S and Graziotti F (2019c) Dataset from dynamic shake-table testing of five full-scale single leaf and cavity URM walls subjected to out-of-plane two-way bending. *Data in Brief* 24: 103854.
- Vaculik J and Griffith MC (2018) Out-of-plane shaketable testing of unreinforced masonry walls in two-way bending. *Bulletin of Earthquake Engineering* 16(7): 2839–2876.